Int. J. Nano Dimens., 7(1): 85-96, Winter 2016
DOI: 10.7508/ijnd.2016.01.010

Research Paper

Experimental investigation on performance comparison of nanofluid-based direct absorption and flat plate solar collectors

S. Delfani [*,1]; *M. Karami* [2]; *M. A. Akhavan Bahabadi* [2]

[1]*Department of Installations, Building and Housing Research Center (BHRC), Tehran, PO Box 13145-1696, Iran*
[2]*School of Mechanical Engineering, College of Engineering, University of Tehran, Tehran, PO Box 14395-515, Iran*

Received 11 May 2015; revised 29 August 2015; accepted 18 September 2015; available online 22 November 2015

ABSTRACT: In the present work, a prototype of a new type of solar collectors called Direct Absorption Solar Collector, was built and its thermal performance is experimentally compared with conventional flat plate solar collector under transient and steady state conditions. Different volume fractions of multi wall carbon nanotubes in water and ethylene glycol mixture (70%: 30% in volume) were used as working fluid of direct absorption solar collector. The transient comparison show that the efficiency of the direct absorption solar collector becomes about 7% (in average) more than that of flat plate solar collector at 72 l/hr flow rate. The steady state performance tests were performed in different flow rates from 54 to 90 l/hr, based on the procedure of EN 12975-2 standard. Under similar operating conditions, a direct absorption solar collector using 100 ppm carbon nanotube nanofluid has the zero-loss efficiency of 23% higher than that of a flat plate collector; whereas, the zero-loss efficiency of a direct absorption solar collector using the base fluid is 4.4% lower than that of a flat plate collector. Based on the results, the performance of a direct absorption solar collector using carbon nanotube nanofluids is better than a flat-plate solar collector.

Keywords: *Carbon nanotubes; Direct absorption solar collector; Flat plate solar collector; Nanofluid; Solar energy.*

INTRODUCTION

In recent years, attempts have been made to absorb more heat from solar radiation in order to enhance the efficiency of the solar collectors, as the main part of residential solar heating systems. Scientists and engineers make effort to enhance the performance of conventional solar collectors by various methods [1]. Using more appropriate working fluids such as nanofluids with better heat transfer characteristics is one of the effective methods to increase the collector efficiency. Studies in this field indicate that utilizing nanofluid in solar systems, offers unique advantages over conventional fluids [2-11]. Yousefi *et al*. [2] investigated the effect of multi wall carbon nanotube (MWCNT)-H_2O nanofluid on the efficiency of flat-plate solar collectors (FPSC) experimentally. They found that the collector efficiency increased substantially by increasing the weight fraction from 0.2% to 0.4%. Also, using the surfactant causes an increase in the efficiency. Jabari Moghadam *et al*. [5] studied the effect of CuO–water nanofluid on the performance and the efficiency of a flat-plate solar collector experimentally. The experimental results of their study reveal that utilizing the nanofluid increases the collector efficiency in comparison to water as an absorbing medium. The nanofluid with mass flow rate of 1 kg/min increases the collector efficiency about 21.8%. Said *et al*. [8] analyzed theoretically entropy generation, heat transfer enhancement capabilities and pressure drop for a flat-plate solar collector operated with single wall carbon nanotubes (SWCNTs) based nanofluids. They observed that the SWCNTs nanofluid reduced the entropy generation by 4.34% and enhanced the heat transfer coefficient by 15.33% compared to water. Pumping power of nanofluid operated solar collector found to be 1.20% higher than the water.

Another effective method to improve the collector efficiency is attention to the concept of direct absorption of incident solar radiation caused introducing of direct absorption solar collector (DASC) in the mid 1970's [12]. In this type of solar collector, the

*Corresponding Author: Shahram Delfani
Email: *delfani@bhrc.ac.ir*
Tel.: (+98) 21 88255942
Fax: (+98) 21 88384171

working fluid absorbs the solar radiation directly (by its volume). By eliminating the tubes and the absorber plate, there is a lower thermal resistance against converting the solar energy into heat, and hence, higher efficiency. The schematic of a direct absorption and a flat plate solar collector are shown in Fig. 1.

By attention to the potential of nanofluids, a new type of direct absorption solar collector (DASC) developed as Nanofluid-based Direct Absorption Solar Collector, firstly investigated numerically by Tyagi *et al*. [13]. They used aluminum nanoparticle suspensions in water as the working fluid and reported the efficiency enhancement of 10% in comparison with a conventional flat plate collector. Otanicar *et al*. [14] have numerically evaluated the performance of low-temperature DASC based on the work of Tyagi *et al*. [13]. They also reported on the experimental results on microsolar direct absorption collector based on nanofluids made from a variety of nanoparticles (carbon nanotubes, graphite, and silver) and demonstrated efficiency improvements of up to 5% by utilizing nanofluids as the absorption mechanism. Parvin *et al*. [15] investigated the heat transfer performance and entropy generation of forced convection through a low-temperature direct absorption solar collector numerically. They found that both the mean Nusselt number and entropy generation increased as the volume fraction of Cu nanoparticles and Reynolds number increase. The economic analysis of Otanicar and Golden [16] indicated that the nanofluid based solar collector has a slightly longer payback period than a conventional solar collector.

Most recently, a prototype of this new type of collector was built with applicability for domestic solar . . . . . *et al*. [17, 18]. They used different volume fractions of copper oxide nanoparticles [17] and functionalized multi wall carbon nanotubes [18] in water and ethylene glycol mixture (70%:30% in volume) as the base fluid. They found that the nanofluids improved the collector efficiency by 9–17% [17] and 10-29% [18] than the base fluid.

Gupta *et al*. [19] investigated the effect of Al_2O_3–H_2O nanofluid flow rate on the efficiency of direct absorption solar collector. Using an experimental setup, they reported that collector efficiency enhancement of 8.1% and 4.2% has been achieved for 1.5 and 2 l/min flow rate of nanofluid, respectively. They also reported the optimum flow rate of 2.5 and 2 l/min towards maximum collector efficiency for water and nanofluid, respectively.

A review of the mentioned literature shows that there are few studies on the thermal performance of nanofluid-based DASC. Also, there is no experimental comparison of the performance of the direct absorption and flat plate solar collectors under similar operating conditions. Taking this into consideration, it has been decided to build a flat plate collector at the same dimensions and features to DASC and modify the DASC experimental setup for comparing the thermal performance of DASC and FPSC based on EN 12975-2 standard, experimentally.

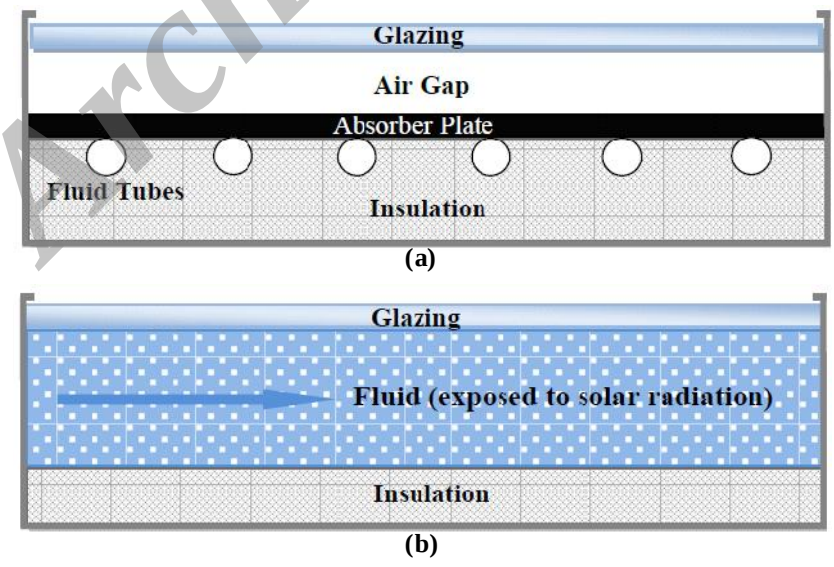

Fig. 1: Schematic of a Direct Absorption Solar Collector (DASC) and a Flat Plate Solar Collector (FPSC).

Multi wall carbon nanotubes in Water/EG (Ethylene Glycol) mixture is used as working fluid of full-scale low-temperature nanofluid-based DASC. The tests were performed in different flow rates from 54 to 90 l/hr for various nanofluid volume fractions.

EXPERIMENTAL

Nanaofluid preparation

In the present work, carboxyl (COOH) functionalized multi wall carbon nanotubes (MWCNT) are suspended in Water/EG mixture (70%:30% in volume) as the base fluid to prepare nanofluids. Nanoparticles with different volume fractions (S1: 0 (base fluid), S2: 25 (0.0525 g/l), S3: 50 (0.105 g/l), S4: 100ppm (0.21 g/l)) were dispersed in the base fluid. The SEM Photography of MWCNTs and the comparative image of nanofluid samples are shown in Fig. 2.

The nanofluid mixture was then stirred and agitated thoroughly for 30min. at 50% amplitude using a 130 W, 20 kHz probe (Hielscher, UP400S, Inc., USA). This ensures uniform dispersion of nanoparticles in the base fluid. Additionally, the mixture is ultrasonicated intermittently (once every 15 min) to avoid overheating. The breaks duration is typically about 2min which provides the opportunity for the energized MWCNTs to dissipate the energy. The procedure of nanofluid preparation assured stability of dispersion at least after a month of preparation [20].

DASC and FPSC

A prototype of DASC was built that measures 60×60 cm^2, with a channel depth of 1cm with applicability for domestic solar heating systems. The main body of the collector was made of aluminum. A manifold with pinholes is used to uniformly entry of working fluid into the channel from the bottom of the collector. Instead of manifold, three holes are considered at the top of the collector to exit the working fluid to avoid increasing the pressure drop. The working fluid flows from the bottom to the top of the collector. The collector glazing of the toughened glass with 4mm thickness is selected due to prevent cracking caused by water pressure. The internal surface of the DASC bottom wall was reflective aluminum for all experiments with nanofluids and one experiment with the base fluid. The internal surface was also black painted to another experiment with the base fluid. All experiments with nanofluids were performed with the reflective internal surface to evaluate only nanofluid absorption ability; whereas the base fluid is tested with both black and reflective internal surfaces. More details of the prototype are available in [17].

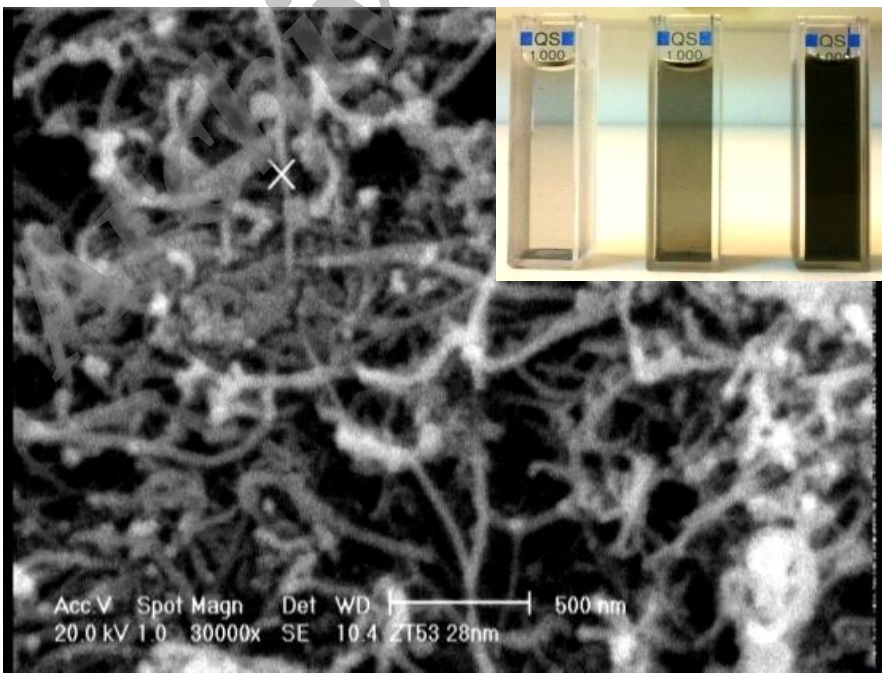

Fig. 2: Scanning electron microscopy (SEM) and image of CNT nanofluids at varying volume fractions (0, 50 and 100 ppm).

A prototype of FPSC was also built at the same dimensions to DASC (cm^2). The absorber plate is from aluminum with 3mm thickness (emissivity: 0.92 and absorptivity: 0.95) and the tubes are from copper (number of tubes: 7, inner and outer diameter of tubes, 10mm and 11mm). The collector glazing is also selected from the toughened glass with 4mm thickness due to similarity to DASC.

Both collectors are insulated within a Polyurethane block of 10mm thickness to limit heat loss from the back and sides of the collectors. The Polyurethane block was shielded from incident radiation with aluminum foil so as to not absorb any of the sunlight.

Test setup and procedure

The collectors were experimentally investigated at the Building and Housing Research Center of Tehran, Iran (latitude is 35.6961° N and longitude is 51.4231° E). The schematic of the test loop based on EN-12975-2 [19] and the photo of the test setup is shown in Fig. 3. The collectors were mounted by tilt angle of 35°to receive maximum solar energy (regarding Tehran latitude). Two electrical pumps and two flow control valves (connected to the water pipe after the electric pump) were used to maintain the flow rate through the collector stable to within 1%.

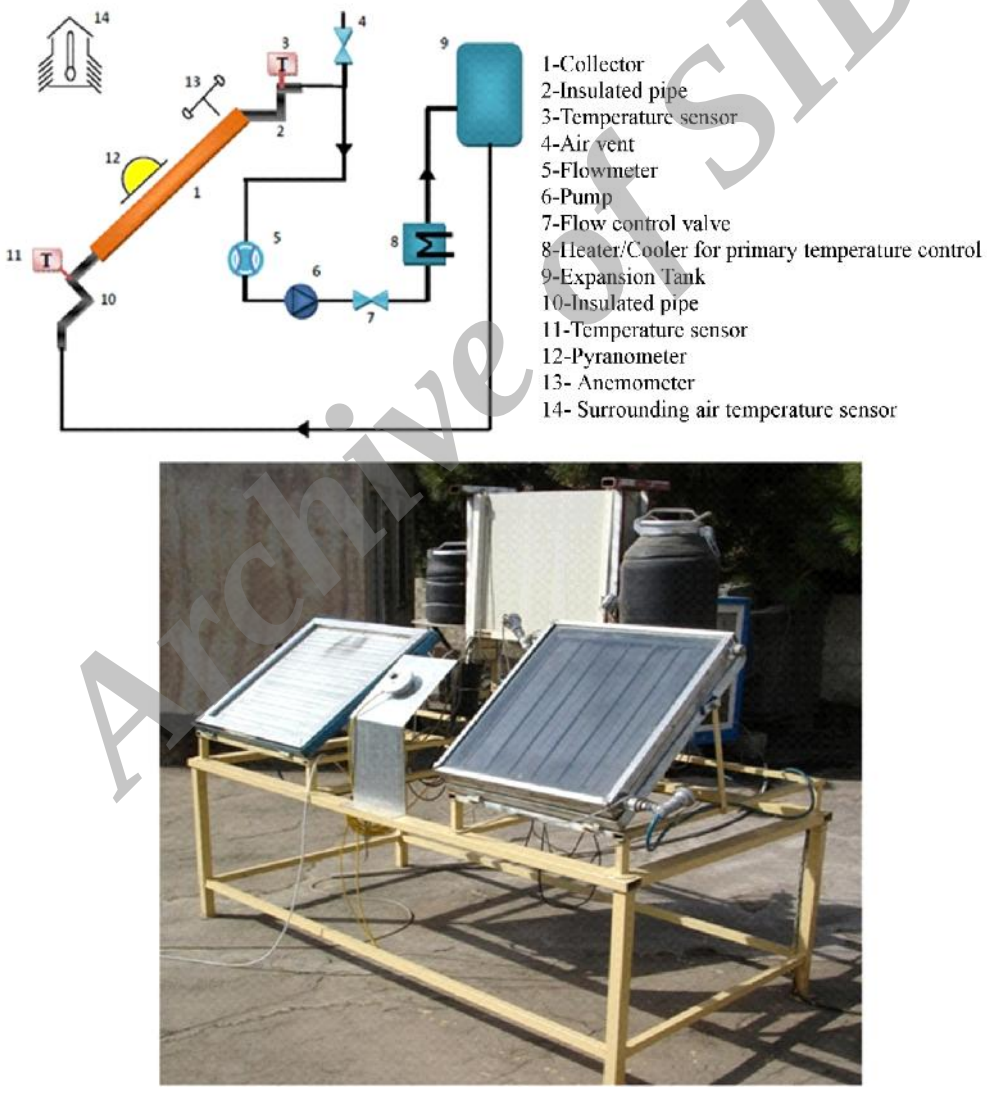

Fig. 3: The schematic of test loop and the experimental setup for DASC and FPSC outdoor performance test.

An expansion tank with about 5 l capacity for DASC and another with 10 l capacity for FPSC were installed, which have been insulated due to reduce heat loss. For primary temperature control, the working fluid was heated or cooled using a heat exchanger to remain inlet temperature constant.

Measuring instruments included two flowmeters which connected to the water pipe before the electric pumps with the ±1% accuracy of the measuring span, four PT100 temperature sensors to measure fluid temperatures in the inlet and outlet of collectors with the accuracy of ± 0.1°C, another temperature sensor to measure the ambient temperature and Kipp&Zonen-CMP6 pyranometer for measuring total solar radiation which its sensor is mounted coplanar, within a tolerance of ±1° with the plane of the collector aperture and TESTO 425 anemometer, recorded ambient air speed by accuracy ± 0.03 *m/s*. A data acquisition system was used to record all measurements.

Calibration of measuring instruments was performed using calibrated references. The temperature sensors were calibrated using a calibrated thermometer to give an uncertainty less than ±0.05°C; the flowmeters using drawing off water from the system into a container and measuring the volume and time with accuracy scales. The uncertainty was about ±2%. The pyranometer and anemometer had a valid calibration certificates with uncertainty of about ±3.5% and ±2.5%, respectively.

The performance of the collectors was compared in both transient and steady state conditions at three different flow rates 54, 72 and 90 l/hr. During the tests, hemispherical solar irradiance, diffuse solar irradiance, air speed, surrounding air temperature, temperature of the heat transfer fluid at the collector inlet and outlet and flow rate of the heat transfer fluid were measured. For transient comparison, the efficiency of the collectors were investigated during an exposure time from 10 a.m. to 15 p.m. The aim was the evaluation of the efficiency variation over the exposure time without draw-off. At the start of the test, the temperature of both collectors was the same. The internal surface of DASC bottom wall was black and the base fluid used as the working fluid of both collectors.

For steady state comparison, the collectors were tested for at least four fluid inlet temperatures over the operating temperature range based on EN 12975-2 standard method. A collector was considered to have been operating in steady-state conditions over a given measurement period if none of the experimental parameters deviate from their mean values over the measurement period by more than the limits given in Table 1 [21].

At least four independent data points were obtained for each fluid inlet temperature, to give a total of 16 data points. The data for each test period were averaged and applied as a single point whereas other data were rejected. The steady state test period included a pre-conditioning period and a steady state measurement period which both of them were at least 4 times the time constant of the collector. The time constant of the collector is defined as the elapsed time in which the fluid outlet temperature arrives 63.2% of its final increase. The collector time constants testing for the FPSC and DASC with the f1 sample are presented in Fig. 4 (a and b), respectively. According to this Figure, the resulted time constant is 3.5 min for FPSC and 4.7 min for DASC. For other working fluids and two internal surfaces of DASC, the time constants ranged from 5–6 min. The higher time constant of DASC is because of more amount of working fluid (about 3.6 l) that is exposed to the ambient during the test than that of FPSC (about 0.3 l).

Efficiency calculation and error analysis

The useful energy extracted can be calculated after the inlet and outlet fluid temperatures and the flowrate of working fluid were measured, using Eq. (1):

$$\dot{Q} = \dot{m} c_p \, \Delta T \tag{1}$$

Table 1: Permitted deviation of measured parameters during a measurement period [21].

Parameter	Permitted deviation from the mean value
Global test solar irradiance	$\pm 50\ W/m^2$
Surrounding air temperature	$\pm 1.5K$
Fluid mass flow rate	$\pm 1\%$
Fluid temperature at the collector inlet	$\pm 0.1K$
Fluid temperature at the collector outlet	$\pm 0.1K$

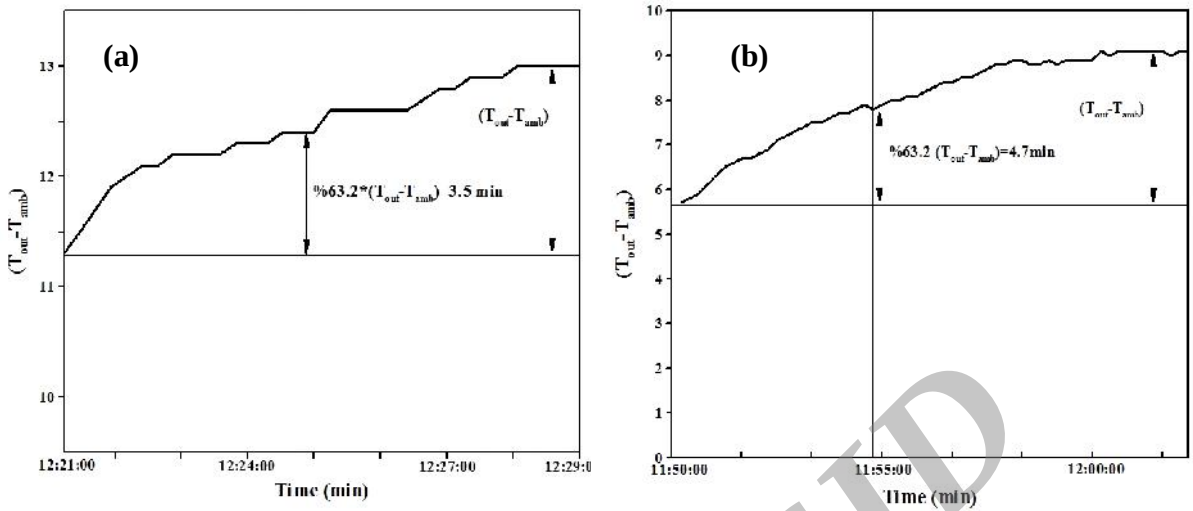

Fig. 4: Collector time constant of (a) FPSC (b) DASC.

The instantaneous collector efficiency (η_i) relates the useful energy to the total radiation incident on the collector surface (AG_T) by Eqs. (2):

$$\eta_i = \frac{\dot{Q}}{AG_T} = \frac{\rho \dot{V} c_p (T_{out} - T_{in})}{AG_T} \quad (2)$$

where $\dot{V}$ is the volumetric flowrate, ρ and c_p are the density and heat capacity of working fluid.

Table 2 shows the corresponding experimentally determined thermophysical properties of the MWCNT nanofluids. The density of the nanofluids was obtained using Pycnometer method (ASTM D-1217) [22], whereas, the ASTM standard test method (E1269-05) [23] was followed to obtain the specific heat () using a differential scanning calorimeter (DSC) (SETARAM, DSC131). As expected, the thermophysical properties are not significantly affected by the addition of nanoparticles, as expected for such low volume fractions.

$$\eta = \eta_0 - a_1 T_{in}^* - a_2 G_T (T_{in}^*)^2 \quad (3)$$

where T_{in}^* is the reduced temperature difference and calculated as:

$$T_{in}^* = \frac{T_{in} - T_{amb}}{G_T} \quad (4)$$

The intersection of the line with the vertical efficiency axis equals to η_0 which called zero-loss efficiency. At this point the temperature of the fluid entering the collector equals to the ambient temperature and collector efficiency is maximum. The slope of the line (a_1) indicates removed energy rate from the solar collector which called heat loss coefficient. The coefficient a_2 shows temperature dependence of the heat loss coefficient [21]. If the value deduced for is negative, a second-order fit shall not be used.

Error analysis for experimental results presented in this study ("steady-state" collector efficiency) has been performed using the method proposed by Abernethy *et al.* [24]:

$$U_{\eta_i} = \sqrt{U_{\dot{m}}^2 + U_{G_T}^2 + U_{\Delta T}^2} \quad (5)$$

where $U_{\dot{m}}^2$, $U_{G_T}^2$ and $U_{\Delta T}^2$ are the uncertainties of $\dot{m}$, G_T and ΔT, respectively, all of which are expressed in percent (i.e., relative error with respect to the average values) and each consists of fixed error which is caused by error of the measuring equipments and random error which is caused by data scattering due to random fluctuation of the process:

$$U_i = \sqrt{U_{i,f}^2 + U_{i,r}^2} \quad (6)$$

$U_{i,f}^2$ represents the fixed error of the *i*th component; $U_{i,r}^2$, represents the random error of the *i*th component. The maximum uncertainty obtained in the present study in determining the collector efficiency, η_i (Eq. (2)), at various tests was around 4.7% for DASC and 6.3% for FPSC (including both fixed and random errors).

Table 2: Thermophysical properties of CNT nanofluid.

Sample	Volume fraction (ppm)	Density (kg/m^3)	Heat Capacity (J/kgK)
S1	0	1043.32	3674.39
S2	25	1043.33	3674.48
S3	50	1043.37	3674.75
S4	100	1043.35	3674.92

RESULTS AND DISCUSSION

Transient Comparison

In this test, the volumes of water circulated in both types of collectors were equal. Since the content of water for filling the FPSC was less that the DASC, the expansion tank of the FPSC had the larger volume than that of the expansion tank of DASC. As mentioned earlier, no water consuming is considered in this test.

Fig. 5 (a) shows the variation of the solar radiation and the ambient temperature over the exposure time from 10 a.m. to 15 p.m. Fig. 5 (b) shows the variation of the outlet temperature of both collectors at 54 l/hr flow rate. As can be seen, the outlet temperature of DASC is higher than that of FPSC at first two hours and then, the trend becomes reversed because of more heat loss from DASC to the ambient at high temperatures. This trend is similar for other flow rates.

The variation of the efficiency at 54 l/hr flow rate is shown in Fig. 5 (c). The results show that, initially, the efficiency of the collectors is approximately equal. However, as the exposure time increased, the efficiency of DASC becomes about 5% (in average) more than that of FPSC. This is due to increase of solar radiation by the time and hence, more solar absorption within the working fluid of DASC. The efficiency enhancement of 7% and 8% is found for 72 and 90 l/hr, respectively. From Fig. 5 (b and c), it is also found that the FPSC has the higher outlet temperature and lower efficiency that the DASC, after 12:00. This is because the FPSC has the higher inlet temperature which is due to more water in its expansion tank.

Steady State Comparison

The steady state tests have performed around solar noon when the hemispherical solar irradiance is greater than 700 W/m^2, diffuse solar irradiance is less than 30% and the average value of air speed is 2-4 *m/s*. Each test was repeated in several days and the best experimental data has been chosen. The experimental results are presented in the form of graphs that describe the collector efficiency against the reduced temperature difference ($\frac{T_{in}-T_{amb}}{G_T}$).

Fig. 6 presents the variations of FPSC efficiency at various flow rates, 54, 72, and 90 l/hr. Since the reduced temperature difference is the ratio of heat loss to solar energy intercepted by the collector; the collector efficiency reduced by increasing the reduced temperature difference, as can be seen in Fig. 6.

It is also found from Fig. 6 that the efficiency increases with flow rate; so that, the zero-loss efficiency at 90l/hr is 17.8% higher than that at 54 l/hr. At low flow rates, the time delay between the entry and exit of working fluid into and out of the collector, i.e. the fluid residence time, is high, allowing for the fluid temperature to rise more. Since heat loss to the ambient including convective and radiative loss increased by temperature (especially, radiation heat loss from the fluid scales with the fourth power of temperature), the fluid suffered higher losses at lower flow rates, which resulted in smaller collector efficiencies. At higher flow rates, the temperature rise in the fluid is small. This resulted in a progressively weaker effect of heat losses described above, and hence, collector efficiencies were seen to be larger at higher flow rates.

Fig. 7 (a and b) present the variations of DASC efficiency with the base fluid as the working fluid and reflective and black internal surfaces, respectively. As can be seen, the DASC efficiency is higher using the black internal surface, because any radiation reaching the bottom wall was absorbed by it, when the bottom wall is black or perfect absorber. This caused the temperature of the bottom wall to rise significantly, and that of the fluid in its vicinity. This resulted in a higher mean fluid temperature at the collector exit, and hence a higher collector efficiency.

The variation of the efficiency by increasing the flow rate is similar to that of the FPSC, shown in Fig. 6.

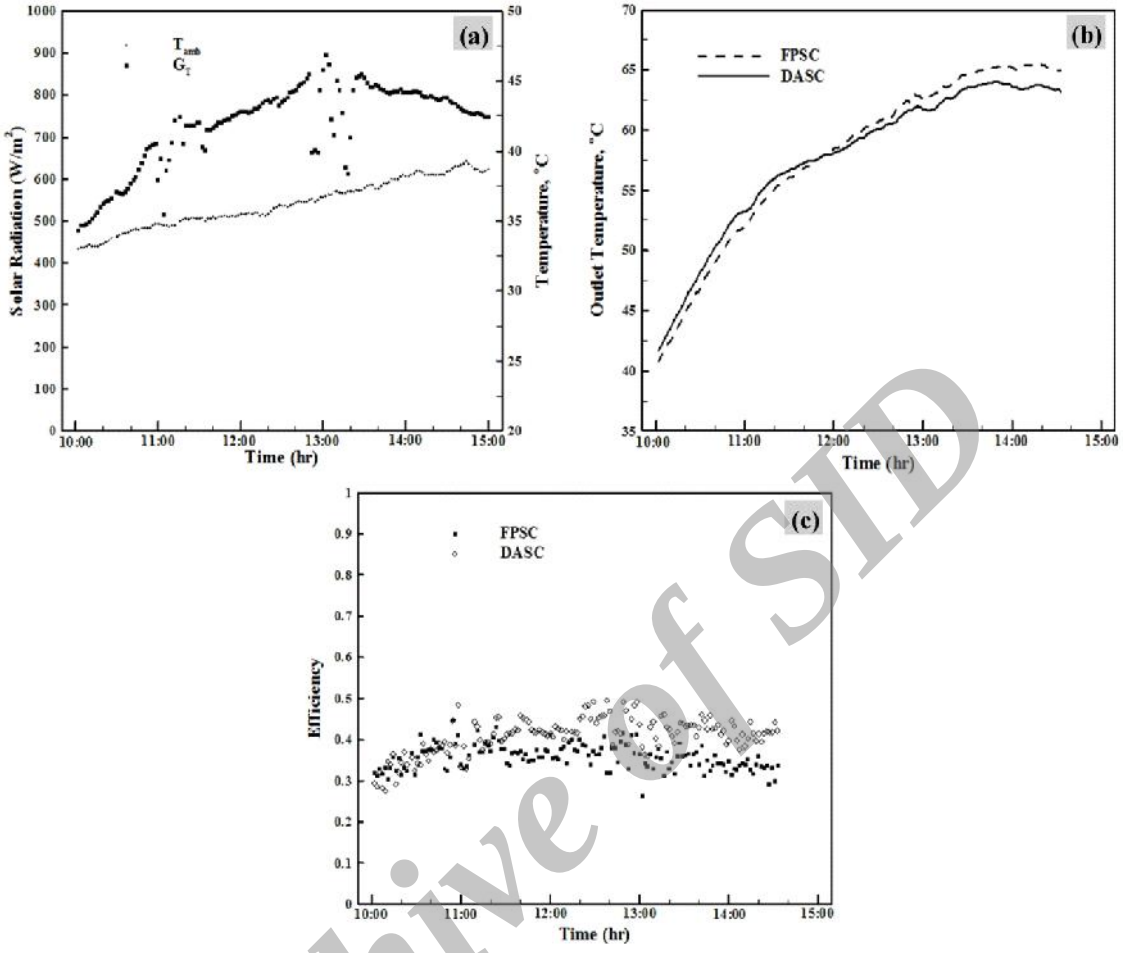

Fig. 5: Variation of (a) solar radiation and ambient temperature (b) collector outlet temperature (c) collector efficiency versus time at 54 l/hr.

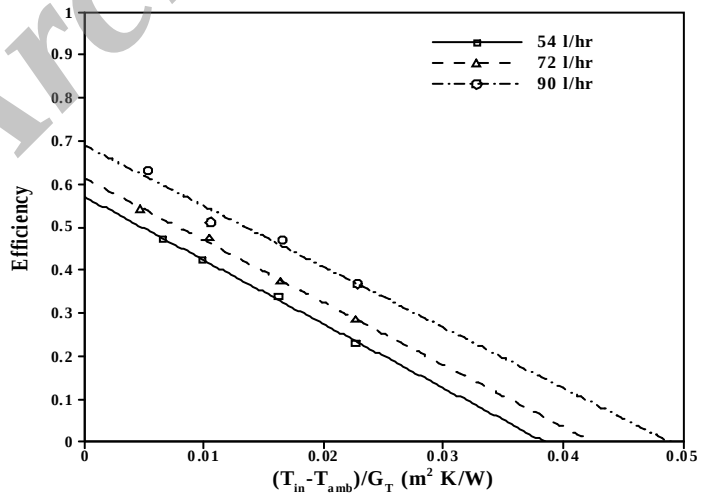

Fig. 6: Efficiency of FPSC at various flow rates.

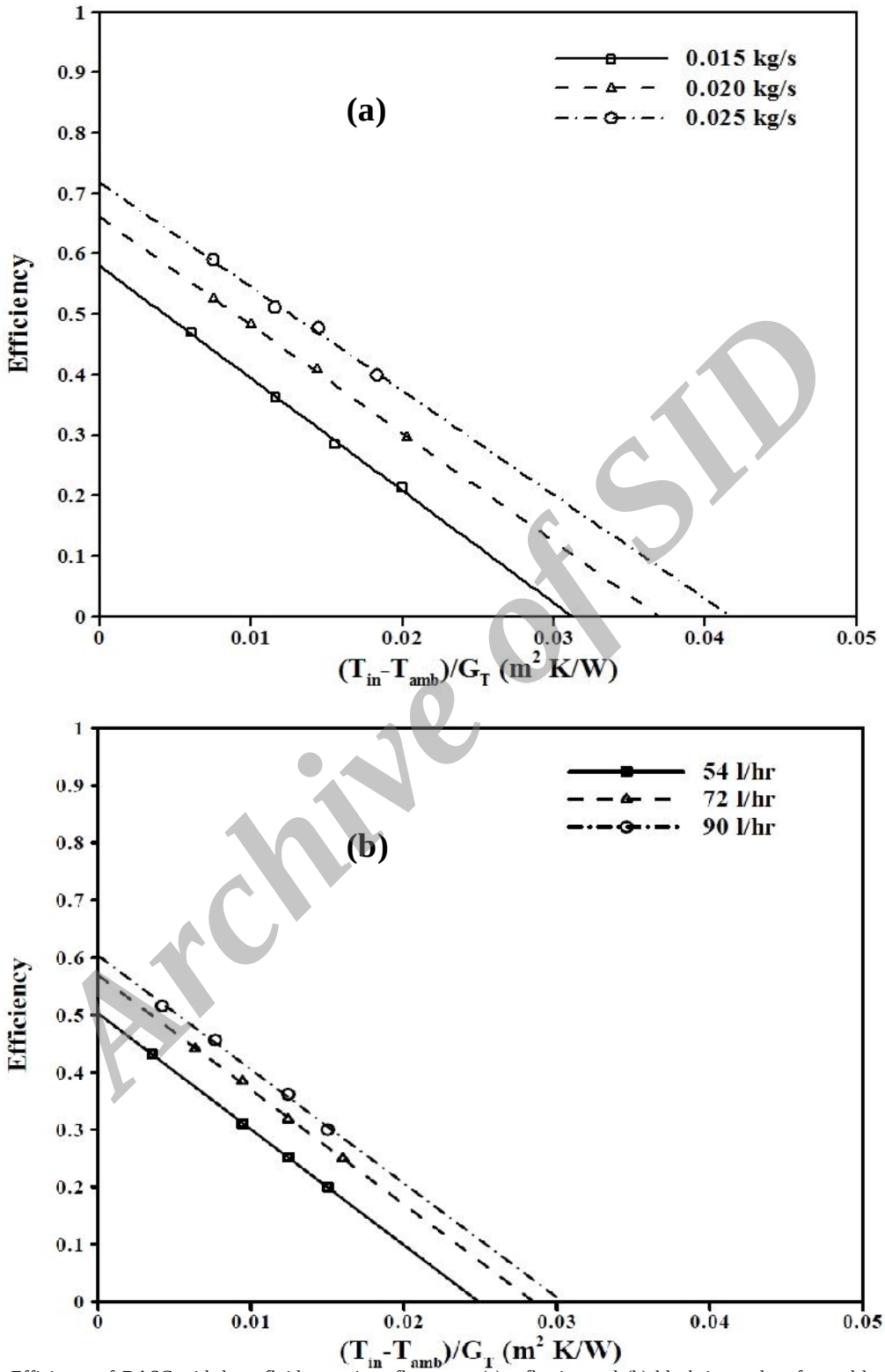

Fig. 7: Efficiency of DASC with base fluid at various flow rates (a) reflective and (b) black internal surface od bottom wall.

It can be concluded from Fig. 7 that the zero-loss efficiency enhancement with flow rate variation from 54 l/hr to 72 l/hr (6.7% by reflective and 5% by black internal surface) is larger than the enhancement with flow rate variation from 72 l/hr to 90 l/hr (3.4% by reflective and 5% by black internal surface). This confirms that the DASC efficiency enhancement has asymptotic trend with increasing of flow rate.

Comparison of DASC and FPSC efficiency with the base fluid as working fluid at 72 l/hr is illustrated in Fig. 8. As mentioned earlier, the experiments with the base fluid were performed with both reflective and black internal surface of DASC bottom wall. As can be seen, the zero-loss efficiency of FPSC is about 4.4% higher than that of DASC with using the base fluid and reflective internal surface; whereas, it is 4.7% lower than that of DASC with using the base fluid and black internal surface.

It is also observed from Fig. 8 that DASC efficiency using the black internal surface is higher than FPSC efficiency in the low reduced temperature difference (<0.013 m^2K/W) and then, the trend becomes reversed, because the heat loss of DASC to the ambient increases more than FPSC at higher temperatures. It can be concluded that DASC has the higher efficiency than FPSC, even using the base fluid, however at low reduced temperature differences.

The efficiency of DASC using CNT nanofluids and FPSC using the base fluid is also compared in Fig. 9. It can be resulted from this Fig. that at constant flow rate, the absorption of solar energy within the nanofluid is increased by increasing nanofluid volume fraction and thus, the collector efficiency is enhanced. Improvement of zero-loss efficiency (η_0) of up to 11.7%, 16.2% and 23% by utilizing S2, S3 and S4 nanofluid samples is demonstrated than to the FPSC, respectively. However, at the higher reduced temperature difference, the heat loss from DASC becomes more, and hence, the efficiency of FPSC were seen to be larger than that of DASC. These results confirm that the performance of the nanofluid-based DASC is better than the FPSC, especially at the low reduced temperature difference.

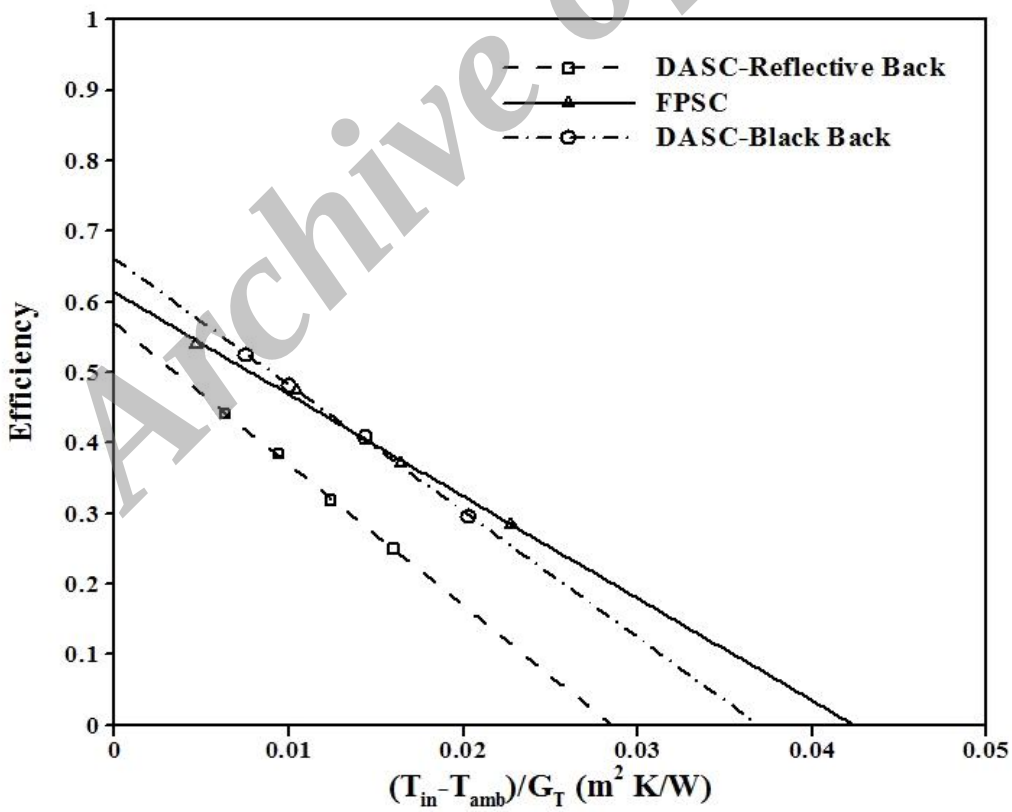

Fig. 8: Comparison of FPSC and DASC efficiency with base fluid as working fluid at 72 l/hr.

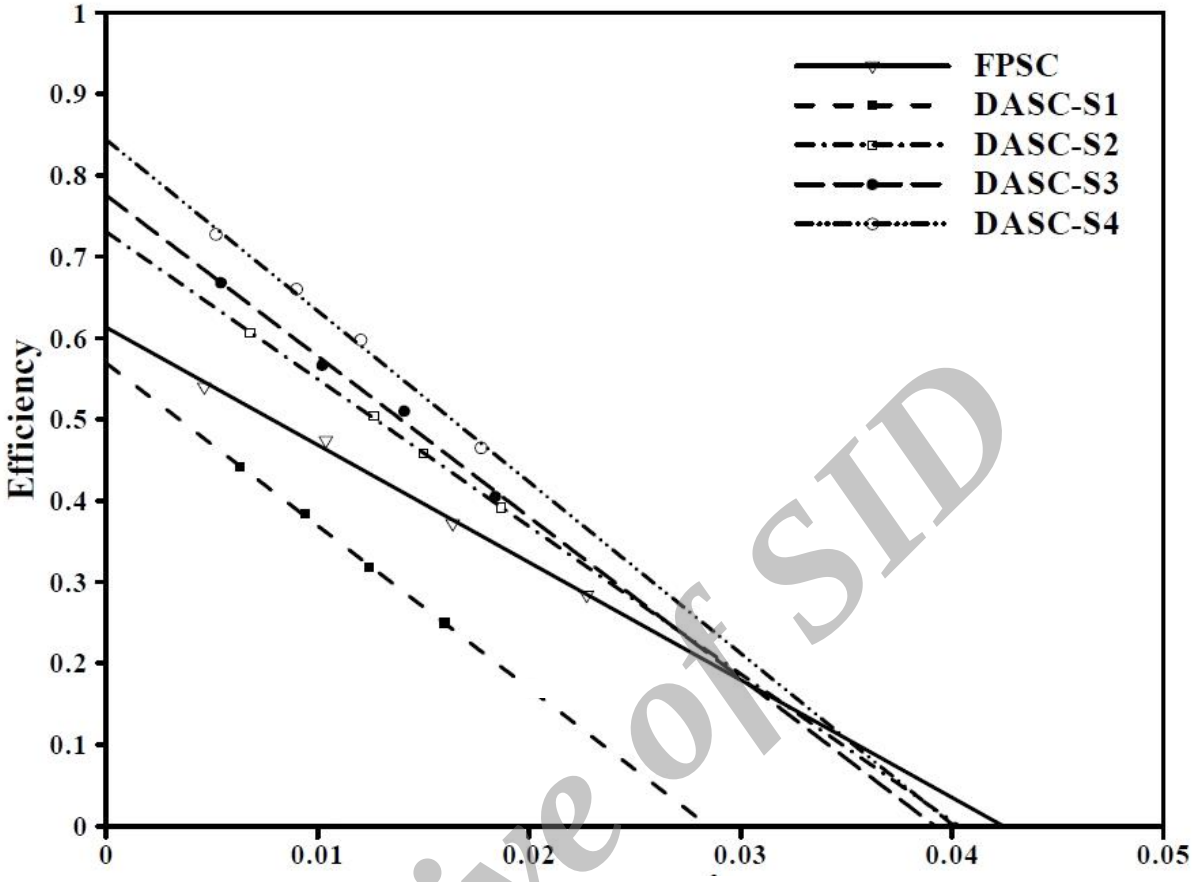

Fig. 9: Comparison of FPSC and DASC efficiency at 72 l/hr.

CONCLUSION

The thermal performance of nanofluid-based direct absorption solar collector and flat plate solar collector was compared experimentally, in both transient and steady state conditions at different flow rates. The results of the comparison lead to the following conclusions:

The transient comparison show that the efficiency of DASC becomes about 5% (in average) more than that of FPSC at 54 l/hr flow rate.

The results of steady state comparison show that the zero-loss efficiency of a FPSC is 4.4% higher and 4.7% lower than that of a DASC using the base fluid with reflective and black internal surface, respectively.

At low reduced temperature differences, DASC has the higher efficiency than that of FPSC, even using the base fluid as the working fluid, when the internal surface of DASC bottom wall is black or perfect absorber.

DASC efficiency using 25, 50 and 100 ppm carbon nanotubes nanofluid is about 11.7%, 16.2% and 23% higher than that of a flat plate collector, under similar operating conditions.

Based on the results, the performance of a direct absorption solar collector (DASC) using carbon nanotubes nanofluids is better than a flat-plate solar collector (FPSC), especially at the low reduced temperature difference.

ACKNOWLEDGMENT

The authorswould like to express their thanks to the Department of Building Installations, Road, Housing and Urban Development Research Center (BHRC) (No. 2012-1313) for the financial supports through the set-up construction and research implementation and also the Center of Excellence in Design and Optimization of Energy Systems, College of Engineering, University of Tehran.

REFERENCES

[1] Javadi F. S., Saidur R., Kamalisarvestani M., (2013), Investigating performance improvement of solar collectors by using nanofluids. *Renew. Sust. Energy Rev.* 28: 232–245.

[2] Yousefi T., Veisy F., Shojaeizadeh E., Zinadini S., (2012), An experimental investigation on the effect of MWCNT-H_2O nanofluid on the efficiency of flat-plate solar collectors. Exper. Thermal and Fluid Sci. 39: 207-212.

[3] Yousefi T., Veisy F., Shojaeizadeh E., Zinadini S., (2012), An experimental investigation on the effect of Al2O3-H_2O nanofluid on the efficiency of flat-plate solar collectors. Renew. Energy. 39: 293-298.

[4] Ghasemi S. E., Mehdizadeh Ahangar GH. R., (2014), Numerical analysis of performance of solar parabolic trough collector with Cu-Water nanofluid. *Int. J. Nano Dimens.* 5: 233-240.

[5] Jabari Moghadam A., Farzane-Gord M., Sajadi M., Hoseyn-Zadeh M., (2014), Effects of CuO/water nanofluid on the efficiency of a flat-plate solar collector. Exper. Thermal and Fluid Sci. 58: 9-14.

[6] Sagadevan S., Pandurangan K., (2015), Investigations on structural and electrical properties of Cadmium Zinc Sulfide thin films. *Int. J. Nano Dimens.* 6: 433-438.

[7] Faizal M., Saidur R., Mekhilef S., Alim M. A., (2013), Energy, economic and environmental analysis of metal oxides nanofluid for flat-plate solar collector. *Energy Conv. Manag.* 76: 162–168.

[8] Said Z., Saidur R., Rahim N. A., Alim M. A., (2014), Analyses of exergy efficiency and pumping power for a conventionalflat plate solar collector using SWCNTs based nanofluid. *Energy and Buildings.* 78: 1–9.

[9] Zamzamian A. M., Keyanpour Rad M., Kiani Neyestani M., Tajik Jamal-Abad M., (2014), An experimental study on the effect of Cu-synthesized/EG nanofluid on the efficiency of flat-plate solar collectors. Renew. Energy. 71: 658-664.

[10] Goudarzi K., Nejati F., Shojaeizadeh E., Asadi Yousef-abad S. K., (2015), Experimental study on the effect of pH variation of nanofluids on the thermal efficiency of a solar collector with helical tube. Exper. *Thermal and Fluid Sci.* 60: 20–27.

[11] Mahian O., Kianifar A., Sahin A. Z., Wongwises S., (2014), Entropy generation during Al_2O_3/water nanofluid flow in a solar collector: Effects of tube roughness, nanoparticle size, and different thermophysical models. *Int. J. Heat and Mass Trans.* 78: 64–75.

[12] Minardi J. E., Chuang H. N., (1975), Performance of a "black" liquid flat-plate solar collector. *Solar Energy.* 17: 179-183.

[13]Tyagi H., Phelan P., Prasher R. S., (2007), Predicted Efficiency of Nanofluid- Based Direct Absorption Solar Receiver. *J. Sol. Energy – Trans.* ASME 131.

[14] Otanicar T. P., Phelan P. E., Prasher R. S., Rosengarten G., Taylor R. A., (2010), Nanofluid-based direct absorption solar collector. *J. Renew. Sustain.* 2: 033102.

[15] Parvin S., Nasrin R., Alim M. A., (2014), Heat transfer and entropy generation through nanofluid filled direct absorption solar collector. Int. J. Heat and Mass Trans. 71: 386–395.

[16] Otanicar T. P., Golden J. S., (2009), Comparative Environmental and Economic Analysis of Conventional and Nanofluid Solar Hot Water Technologies. *Environ. Sci. Technol.* 43: 6082–6087.

[17] Delfani S., Karami M., Akhavan Bahabadi M. A., Raisee M., (2015), Experimental Investigation of CuO Nanofluid-based Direct Absorption Solar Collector for Residential. Appl. *Renew. Sustainable Energy Rev. J.* 29: 1-10.

[18] Karami M., Delfani S., Akhavan Bahabadi M. A., (2016), Performance Characteristics of a Residential-type Direct Absorption Solar Collector using MWCNT Nanofluid. *Renew. Sustainable Energy.* 87: Inpress.

[19] Gupta H. K., Agrawal G. D., Mathur J., (2015), Investigations for effect of Al2O3–H2O nanofluid flowrate on the efficiency of direct absorption solar collector. *Case studies in therm. eng.* 5: 70-78.

[20] Karami M., Akhavan Bahabadi M. A., Delfani S., Ghozatloo A., (2014), A new application of carbon nanotubes nanofluid as working fluid of low-temperature direct absorption solar collector. *Solar Energy Mat. Solar Cells.* 121: 114–118.

[21] Thermal solar systems and components – Solar collectors – Part 2: Test methods, English version of DIN EN 12975-2: 2006-06.

[22] ASTM D1217-12, Standard Test Method for Density and Relative Density (Specific Gravity) of Liquids by Bingham Pycnometer, 2012.

[23] ASTM E1269 – 11, Standard Test Method for Determining Specific Heat Capacity by Differential Scanning Calorimetry, 2011.

[24] Abernethy R. B., Benedict R. P., Dowdell R. B., (1983), ASME measurement uncertainty. ASME paper 83-WA/FM-3.

How to cite this article: (Vancouver style)

Delfani Sh., Karami M., Akhavan Bahabadi M. A., (2016), Experimental investigation on performance comparison of nanofluid-based direct absorption and flat plate solar collectors. *Int. J. Nano Dimens.* 7(1): 85-32.

DOI: 10.7508/ijnd.2016.01.010

URL: http://ijnd.ir/article_15588_2444.html